

# Chemometrical approach to the determination of the fractal dimension(s) of real objects

Volodymyr V. Kindratenko, Boris A. Treiger, Pierre J.M. Van Espen \*

*Micro- and Trace Analysis Center (MiTAC), Department of Chemistry, University of Antwerp (UIA), B-2610 Antwerp, Belgium*

Received 15 September 1995; revised 5 January 1996; accepted 5 January 1996

---

## Abstract

Fractal dimension has been recognized for a long time as a useful parameter for shape characterisation. However, the use of the fractals concept requires the visual inspection of the Richardson plot which hampers the practical applications. In this paper a fully automatical method for the analysis of the Richardson plot is described. A clustering approach is adopted instead of the visual inspection of Richardson plot. Cases which explain the application of the method are examined.

*Keywords:* Fractal dimensions; Shape characterization

---

## 1. Introduction

The concept of fractals was originally introduced in one of the earlier papers by Mandelbrot [1] in which he tried to resolve the paradox encountered by Richardson in his attempt to answer the question ‘how long is the coastline of Great Britain’. The answer to this question essentially seems to depend on the yardstick used to measure the length of the coastline. Richardson observed that if the measured coastline was plotted against the size of the yardstick,  $\lambda$ , using logarithmic axes (Richardson plot), the result was a straight line. Furthermore, the slope of the line was different for different boundaries. More irregular coastlines as judged by human observers always result in a line with a higher slope. The slope is negative, since the largest value for the coastline length is

obtained with the shortest yardstick. The magnitude of the slope of the line is between zero and one. The fractal dimension of the coastline is just this magnitude plus 1, the topological dimension of a line.

This concept was found to be useful to determine the fractal dimension of not only the coastlines, but also of different natural objects: aerosol particles, biological cells, etc. It was shown (see, e.g. [2]) that for a variety of objects at various magnifications the data did not follow the ideal straight line (single fractal) expected for a (true) fractal. Practically in all cases the data on a Richardson plot can be satisfactorily explained as two straight line segments having different slopes (bifractals or, in general, multifractals). Kaye’s description of the two line segments of the Richardson plots uses the terms ‘structural’ and ‘textural’ for the two different regions. At fine scales a ‘textural’ dimension is given by the slope of the line at small values of  $\lambda$ , while at large scale the ‘structural’ characteristics of the object emerge.

---

\* Corresponding author.

When a Richardson plot has been constructed (various techniques can be found in [2,3]) it is necessary to fit a straight line to the data to determine the slope (or slopes in the case of a multifractal) and hence the fractal dimension(s). The main difficulty is that, as it has been pointed by Mandelbrot, in the real world any fractal description of a natural boundary would have inspection limits. It means that fractality of a real object can be observed only within some limited intervals of the yardstick sizes. However, it is not always evident where the best straight line segment(s) on the graph occur. Moreover some multifractal objects may show continuous gradients of fractal change [4] and it is not easy to determine where the best breakpoint between two straight lines of the graph is. There are no criteria proposed up to date for preferable breakpoint selection in such cases. Up to our knowledge the straight line segment of a Richardson plot is mainly detected by visual inspection [4–7]. Obviously, this visual line fitting can lead to problems. Here we propose a method which eliminates these difficulties and reveals the correct fractal dimension(s) without visual inspection of a Richardson plot. This procedure allows to fully automate the determination of the fractal dimension. Such automation is important in, e.g., electron microscopic investigation of microscopic particles. In environmental research, the composition and shape of hundreds or thousands of atmospheric aerosol particles are determined. Their fractal dimension, together with their chemical composition is used to identify the particles and to assign them to possible sources [7].

## 2. Theory

The fractal dimension(s) of an object is (are) determined from its digital image (e.g. as obtained with a scanning electron microscope). The object is discriminated from the background by converting the original grey level image into a binary image. Next the contour of the object is obtained using a classical boundary following technique [7], resulting in a set of contour points  $\{x_i, y_i\}$ .

### 2.1. Construction of the Richardson plot

Construction of the Richardson plot involves the determination of the perimeter of the object for vari-

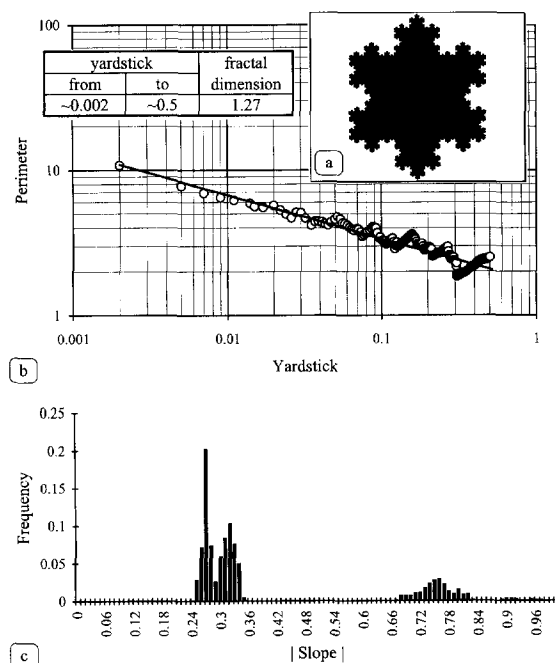


Fig. 1. (a) The triadic Koch island after 5 iterations with theoretical fractal dimension  $\log 4/\log 3 = 1.2618\dots$ ; (b) corresponding Richardson plot (here and in the next figures yardstick and perimeter are shown in fractions of the maximum Feret diameter); (c) the frequency histogram, obtained from the Richardson plot shown ( $k = 4$ ,  $\sigma = 0.01$ ). Its maximum corresponds to a fractal dimension of 1.27.

ous lengths of the yardstick  $\lambda$ . In the Richardson plot the logarithm of the perimeter is plotted against the logarithm of the yardstick length (Fig. 1b).

For a given yardstick size  $\lambda$ , the perimeter of the object is determined as follows. Starting at some arbitrary contour point  $(x_s, y_s)$  the next point on the contour  $(x_n, y_n)$  in clockwise direction is located which has distance  $d_j = \sqrt{(x_s - x_n)^2 + (y_s - y_n)^2}$  as close as possible to  $\lambda$ . This point is then used to locate the next point on the contour that satisfies this condition. The process is repeated until the distance between the last located point and the starting point is less than  $\lambda$ . The perimeter is the sum of all distances  $d_j$  including the distance between the last located point and the starting point. This method is referred to as the 'hybrid' method and is discussed in detail in [8].

The length of the yardstick  $\lambda$  usually varies between 0.001 and 0.5 times the maximum Feret diam-

eter of the object. The maximum Feret diameter is defined as the largest distance between two points of the object.

## 2.2. Automatic extraction of the fractal dimension(s)

Once the Richardson plot has been constructed we have  $n$  points  $(x_i, y_i)$  where  $x$  represents the yardstick length  $\lambda$ ,  $y$  the perimeter and  $n$  the number of data points in the Richardson plot. The statement that there exists a straight line which fits a certain subset of the points implies that there exists a certain inherent structure. The question is then how to reveal this structure. One possible way is to apply a multivariate analysis technique such as cluster analysis (CA), specially intended to solve such types of problems. However, in order to directly apply CA to this specific case, the problem should be reformulated as follows. Let us, instead of all  $n$  points in the plane, consider all possible straight lines each of which fits any ordered subset of  $m$  points from left to right in the plane ( $m = k, k + 1, \dots, n$ , where  $k$  is certain lower limit). Each of these lines is characterised by its slope  $a$  and intercept  $b$ . The best fit values of  $a$  and  $b$  in the least squares sense are calculated as [3]:

$$a = \frac{m \sum_{i=1}^m x_i y_i - \sum_{i=1}^m x_i \sum_{i=1}^m y_i}{m \sum_{i=1}^m x_i^2 - \left( \sum_{i=1}^m x_i \right)^2} \quad (1)$$

$$b = \frac{1}{m} \left( \sum_{i=1}^m y_i - a \sum_{i=1}^m x_i \right) \quad (2)$$

From the point of view of determining the fractal dimension only slope  $a$  is of interest. However, the computation of the expected error in the slope

$$\sigma = \sqrt{\frac{mS}{m \sum_{i=1}^m x_i^2 - \left( \sum_{i=1}^m x_i \right)^2}} \quad (3)$$

where

$$S = \frac{1}{m-1} \left( \sum_{i=1}^m y_i^2 + mb^2 + a^2 \sum_{i=1}^m x_i^2 - 2 \left( b \sum_{i=1}^m y_i - ab \sum_{i=1}^m x_i + a \sum_{i=1}^m x_i y_i \right) \right) \quad (4)$$

involves the calculation of the intercepts too. For the purpose of this application it is logical to consider only those straight lines which have slopes in the interval  $-1$  and  $0$ . Furthermore we restrict ourselves to lines with slope errors  $\sigma$  not exceeding a certain threshold. This results finally in a one-dimensional set containing all possible slopes. The problem of finding the underlying structure through clustering can now be solved via constructing the frequency histogram. The maxima in the histogram show the most populated cluster(s) which correspond to the most appropriate fractal dimension(s).

## 3. Results and discussion

As a first example let us consider the problem of determining the fractal dimension of the triadic Koch island (Fig. 1a) with theoretical fractal dimension  $\log 4 / \log 3 = 1.2618\dots$  [9]. The Richardson plot was constructed (Fig. 1b) by the method briefly described in the theoretical section. The frequency histogram of all possible slopes, calculated as described above (here and in the following examples  $k = 4$ ,  $\sigma \leq 0.01$ ) is shown in Fig. 1c. The maximum of the histogram is reached at  $|a| = 0.27$  which corresponds to the fractal dimension of 1.27 which is in good agreement with the theoretical value.

The book by Mandelbrot [10] contains many examples of the artificial islands having various fractal dimensions. Some of them were analysed by the present method and the following results were obtained. For the smoother Koch island (plate 46 from [10]) having theoretical fractal dimension  $\log 3 / \log \sqrt{7} = 1.1291\dots$  the value 1.14 was obtained. A quadric Koch island (plate 49) was constructed with theoretical fractal dimension 1.5. As the result of analysis by the present method the value of 1.48 was obtained. Finally, a circle (Fig. 2a), which is known to be a non-fractal object in Euclidean geometry, was also analysed. The frequency histogram (Fig. 2c), obtained from the corresponding Richardson plot (Fig. 2b), shows a fractal dimension of 1.01 ( $\pm 0.01$ ) which actually means the absence of fractality.

An agglomerate (Fig. 3a) similar to one of the oldest well known objects with multifractal properties, the Medalia's carbonblack profile [11], was generated and analysed in order to check the applicabil-

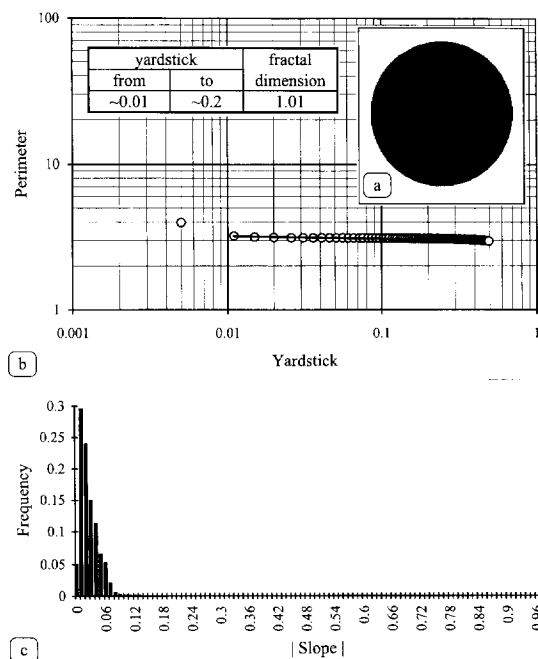


Fig. 2. (a) A non-fractal object (a circle); (b) corresponding Richardson plot; (c) the frequency histogram, obtained from the Richardson plot shown ( $k = 4$ ,  $\sigma = 0.01$ ).

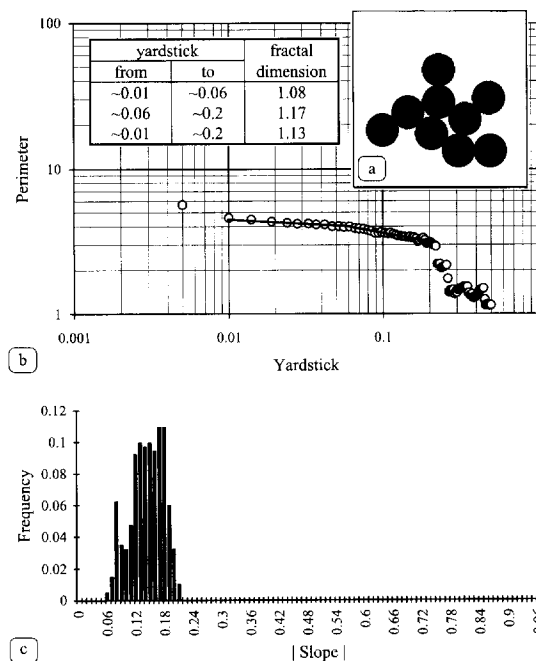


Fig. 3. (a) A synthetic agglomerate profile created from the set of circles (similar to the carbonblack profile); (b) corresponding Richardson plot; (c) the frequency histogram ( $k = 4$ ,  $\sigma = 0.01$ ).

ity of the method for characterising complex multi-fractal objects. The frequency histogram (Fig. 3c) shows a global maximum which reveals a fractal dimension of 1.17. More thorough analysis of the frequency histogram discloses two local maxima which correspond to fractal dimensions of 1.08 and 1.13.

The visual inspection of the Richardson plot (Fig. 3b) shows the two distinct lines (as predicted by our method) which correspond to fractal dimensions of 1.08 (textural) and 1.17 (structural). The value of 1.13 is an average of the textural and structural fractals, measured over the interval  $\lambda = 0.01$  to  $\lambda = 0.20$  (see

Table 1

Known fractal dimensions and value obtained by the present method for some artificially generated and real objects. Here 'known' means 'theoretical' or 'from literature'

Single fractals	Known fractal dimension		Fractal dimension obtained by the present method	
	Textural	Structural	Textural	Structural
Circle (Fig. 2a)		1 (non-fractal)		$1.01 \pm 0.01$
Smoother Koch island [10]		1.1291...		$1.14 \pm 0.01$
Triadic Koch island (Fig. 1a)		1.2618...		$1.27 \pm 0.01$
Quadric Koch island [10]		1.5		$1.48 \pm 0.01$
Coast of Great Britain [14]		ca. 1.3		$1.32 \pm 0.01$
Algae cell (Fig. 4a)		–		$1.04 \pm 0.01$
Multifractals	Textural	Structural	Textural	Structural
Medalia's carbonblack profile [11]	1.10	1.32	$1.13 \pm 0.01$	$1.32 \pm 0.01$
Artificially generated carbonblack profile (Fig. 3a)	–	–	$1.08 \pm 0.01$	$1.17 \pm 0.01$
Algae cells agglomerate (Fig. 5a)	–	–	$1.13 \pm 0.007$	$1.39 \pm 0.01$

Fig. 3b). A similar situation was encountered by Flook [12] and is discussed in Kaye's book [2] using the Medalia's carbonblack profile as an example. Kaye shows the presence of both textural (1.10) and structural (1.32) fractal dimensions and discusses his early studies [13] of the carbonblack profile where an overall fractal dimension of 1.18 was obtained as an averaged. The results of our analysis of the original Medalia's carbonblack profile as it appears in [11] are quite similar to that of Kaye: structural fractal dimension of 1.32; textural fractal dimension of 1.13 and average fractal dimension of 1.19. The results of the discussion are summarised in Table 1 together with some other examples.

All results shown above have been obtained with  $k = 4$  and  $\sigma \leq 0.01$ . It is interesting to inspect the changes of a frequency histogram vs.  $k$  and  $\sigma$ . In order to do this two biological examples were used. Fig. 4 and Fig. 5a show scanning electron microscopy images of individual algae cells and cell agglomerates, respectively. Richardson plots are shown in Fig. 4b and 5b. One straight line on the plot (Fig. 4b) can be observed corresponding to fractal dimension of 1.04. The Richardson plot for the agglomerate of algae cells (Fig. 5b) shows the two straight lines corresponding to textural 1.13 and structural 1.39 fractal dimensions. The frequency histograms were obtained for different values of  $k$  (Fig. 4c and Fig. 5c) and  $\sigma$  (Fig. 4 and Fig. 5d). Both parameters were chosen in intervals from possible smallest to reasonably large numerical values. There is no difference in the position of the global maxima for different values of  $k$  (Fig. 4c and Fig. 5c). With increasing  $k$  some local maxima, however, can be lost (Fig. 5c). Thus, the numerical value of  $k$  should be chosen relatively small in order to obtain a histogram with a lot of detail that can reveal the finest structure in the fractal object. Differences of the histograms for different  $\sigma$  are evident especially in case of multifractal object (Fig. 5d). For relatively small values the maximum of the histogram corresponds to textural fractal dimension. Starting from certain larger values the maximum corresponds to the structural one (Fig. 5d). So, if a relatively small value of  $\sigma$  was chosen the textural fractal dimension can be revealed by the global maximum of a frequency histogram. In the other case the global maximum corresponds to the structural fractal dimension. Usually there is no essential influ-

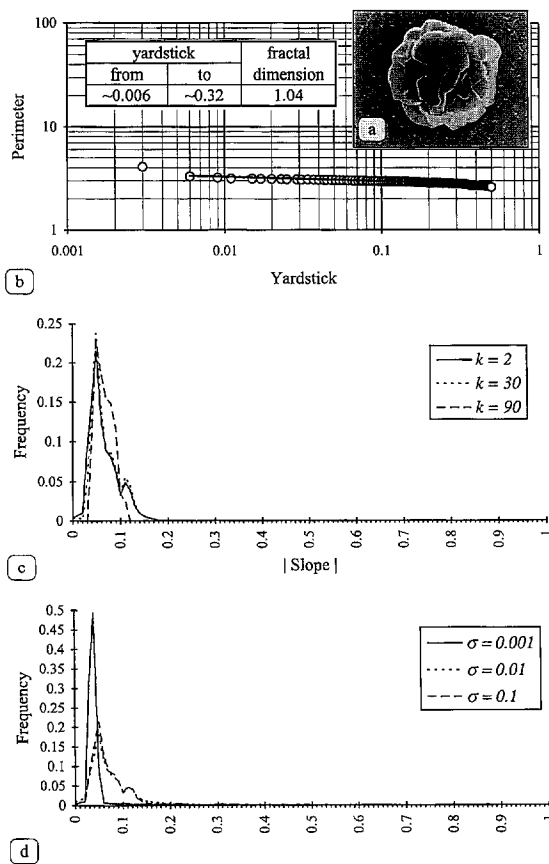


Fig. 4. (a) An individual algae cell; (b) corresponding Richardson plot; (c) the frequency histogram for the parameters  $k = 2$ ,  $k = 30$  and  $k = 90$  ( $\sigma = 0.01$ ); (d) the frequency histogram for the parameters  $\sigma = 0.001$ ,  $\sigma = 0.01$  and  $\sigma = 0.1$  ( $k = 2$ ).

ence of a chosen value of  $\sigma$  on the location of the maximum of the histogram in the cases when only a single line can be observed on a Richardson plot.

As one can see from Fig. 1b, Fig. 2b, Fig. 3b and Fig. 4b all perimeter estimations were performed for rather large intervals of the yardstick sizes until 0.5 of the maximum Feret diameter. Some researchers consider only intervals until ca. 0.3 [2]. The reason of using such a large yardstick-sized interval is that there is no guarantee that the fractal properties of an object can be observed over the interval up to ca. 0.3 times the maximum Feret diameter. Fig. 5b shows an example where the straight line of Richardson plot is observed up to ca. 0.4 times the maximum Feret diameter. Until now we never observed fractal proper-

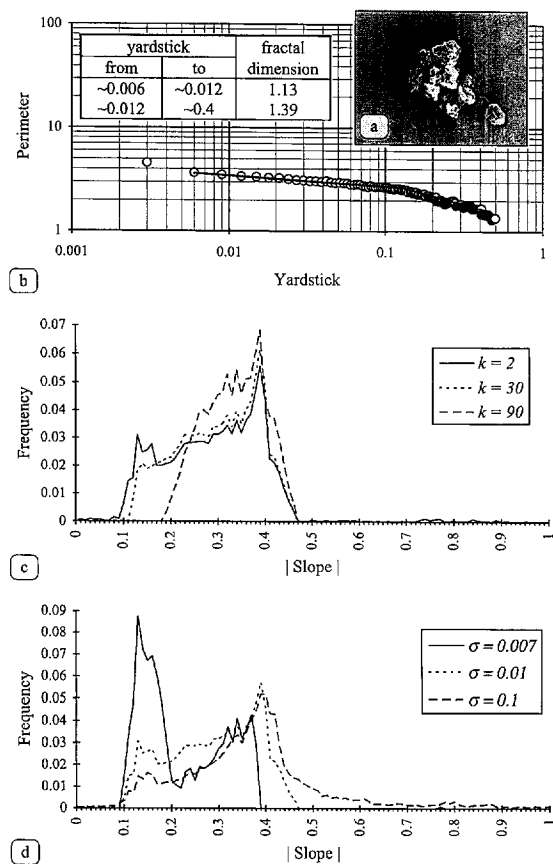


Fig. 5. (a) An agglomerate of algae cells; (b) corresponding Richardson plot; (c) the frequency histogram for the parameters  $k = 2$ ,  $k = 30$  and  $k = 90$  ( $\sigma = 0.01$ ); (d) the frequency histogram for the parameters  $\sigma = 0.007$ ,  $\sigma = 0.01$  and  $\sigma = 0.1$  ( $k = 8$ ).

ties of real objects (not theoretical, like Koch curve) outside the given interval (but this does not mean that they do not exist). Here we use reasonably large yardstick-sized intervals which can completely reveal a fractal dimension.

#### 4. Conclusion

For all studied examples of theoretical and real objects we always found a relation between fractal

dimension of an object and a maximum of a corresponding frequency histogram. Depending on a chosen value of  $\sigma$  a textural or structural fractal dimension can be revealed by the global maximum of the histogram. For a relatively large  $\sigma$  the global maximum corresponds to a structural fractal dimension, whereas for smaller  $\sigma$  it reveals a textural fractal dimension. For single fractal objects the maximum of the histogram doesn't change essentially. In order to reveal the fine structure of the histogram a relatively small value of  $k$  should be selected. For most examples discussed above we chose  $k$  equal to 4 and  $\sigma$  equal to 0.01 for determining a structural fractal dimension.

The proposed approach opens the way to automatic calculation of fractal dimensions from the corresponding Richardson plot data.

#### References

- [1] B.B. Mandelbrot, *Science*, 155 (1967) 636–638.
- [2] B.H. Kaye, *A Random Walk through Fractal Dimensions*, VCH Verlagsgesellschaft, Weinheim, 1986, pp. 13–52.
- [3] J.C. Russ, *Fractal Surfaces*, Plenum Press, New York, 1994, pp. 27–57.
- [4] J.D. Orford and W.B. Whalley, *Sedimentology*, 30 (1983) 655–668.
- [5] H. Schwarz and H.E. Exner, *Powder Technol.*, 27 (1980) 207–213.
- [6] Y.Xie and P.K. Hopke, *Aerosol Sci. Technol.*, 20 (1994) 161–168.
- [7] V.V. Kindratenko, P.J.M. Van Espen, B.A. Treiger, R.E. Van Grieken, *Environ. Sci. Technol.*, 28 (1994) 2197–2202.
- [8] N.N. Clark, *Powder Technol.*, 46 (1986) 45–52.
- [9] K. Falconer, *Fractal Geometry: Mathematical Foundations and Applications*, John Wiley, New York, 1990, pp. xiii–xxii.
- [10] B.B. Mandelbrot, *Fractals: Form, Chance and Dimension*, Freeman, San Francisco, 1977.
- [11] A.I. Medalia and G.J. Hornik, *Pattern Recognition*, 4 (1975) 155.
- [12] A.G. Flook, *Powder Technol.*, 21 (1978) 295–298.
- [13] B.H. Kaye, *Powder Technol.*, 21 (1978) 1–16.
- [14] J. Feder, *Fractals*, Plenum Press, New York, 1988, p. 9.